LETTER

https://doi.org/10.1038/s41586-018-0399-1

Ecosystem warming extends vegetation activity but heightens vulnerability to cold temperatures

Andrew D. Richardson[1,2,3]*, Koen Hufkens[1], Thomas Milliman[4], Donald M. Aubrecht[1], Morgan E. Furze[1], Bijan Seyednasrollah[1,2,3], Misha B. Krassovski[5], John M. Latimer[5], W. Robert Nettles[5], Ryan R. Heiderman[5], Jeffrey M. Warren[5] & Paul J. Hanson[5]

Shifts in vegetation phenology are a key example of the biological effects of climate change[1–3]. However, there is substantial uncertainty about whether these temperature-driven trends will continue, or whether other factors—for example, photoperiod—will become more important as warming exceeds the bounds of historical variability[4,5]. Here we use phenological transition dates derived from digital repeat photography[6] to show that experimental whole-ecosystem warming treatments[7] of up to +9 °C linearly correlate with a delayed autumn green-down and advanced spring green-up of the dominant woody species in a boreal *Picea–Sphagnum* bog. Results were confirmed by direct observation of both vegetative and reproductive phenology of these and other bog plant species, and by multiple years of observations. There was little evidence that the observed responses were constrained by photoperiod. Our results indicate a likely extension of the period of vegetation activity by 1–2 weeks under a 'CO_2 stabilization' climate scenario (+2.6 ± 0.7 °C), and 3–6 weeks under a 'high-CO_2 emission' scenario (+5.9 ± 1.1 °C), by the end of the twenty-first century. We also observed severe tissue mortality in the warmest enclosures after a severe spring frost event. Failure to cue to photoperiod resulted in precocious green-up and a premature loss of frost hardiness[8], which suggests that vulnerability to spring frost damage will increase in a warmer world[9,10]. Vegetation strategies that have evolved to balance tradeoffs associated with phenological temperature tracking may be optimal under historical climates, but these strategies may not be optimized for future climate regimes. These in situ experimental results are of particular importance because boreal forests have both a circumpolar distribution and a key role in the global carbon cycle[11].

In temperate and boreal regions, rising temperatures are advancing spring onset (for example, budburst and flowering) and delaying autumn senescence (for example, leaf coloration and leaf fall)[12,13]. Whether these trends will be maintained is an open question[4]. Warm and cold temperatures, photoperiod and insolation, and precipitation and water availability have all been shown to influence plant phenology[2,5,14,15]. However, the future response of phenology to rising temperatures still remains largely unknown because of the high degree of uncertainty associated with interactions among these drivers[12]. Importantly, it has previously been proposed that photoperiod may constrain the phenological response to rising air temperatures[4,5,16]. Although there is evidence for this in some species[8,15], the generality of these results—and whether there are robust patterns across functional types—has yet to be demonstrated[5].

Analyses of observational datasets to disentangle the effects of these drivers are challenged by the lack of variability in natural systems, the inherent correlation among drivers and the realism of space-for-time assumptions[12]. Experimental approaches are thus required. However, there are sizable challenges associated with conducting realistic environmental manipulations, particularly for ecosystems with tall vegetation. Because of financial, logistical and technological hurdles, experimental warming treatments have not previously been applied to forest stands, and have only rarely been applied to single mature trees[17]. Although experiments with seedlings and branch cuttings are relatively common[18,19], artefacts associated with these approaches may limit their broader applicability[20,21].

We have been studying the effect of experimental whole-ecosystem warming treatments on vegetation phenology at the 'Spruce and Peatland Responses Under Changing Environments' (SPRUCE) facility, a long-term, multi-factor manipulative experiment situated in a boreal peatland forest in the Upper Midwest of the United States[7]. To our knowledge, this experiment is unique in that the five levels of warming (from 0 to +9 °C, see Methods, Extended Data Fig. 1, Supplementary Note 1, Extended Data Table 1) are being applied to intact communities of native plants, including woody shrubs and mature trees. The dominant plant species at SPRUCE represent key genera that are found across the vast boreal forest (taiga), which covers much of the land surface of the Northern Hemisphere from 45° to 70° N. Knowledge of the environmental controls on the phenology of these species is poor and does not at present provide a strong basis for making predictions about the capacity for phenological tracking of a warmer climate. Results from SPRUCE will therefore inform our understanding of the effects of climate change on processes related to biogeochemical cycling and biosphere–atmosphere feedbacks for this globally extensive biome.

Our focus here is on the effect of the experimental ecosystem warming treatments on spring and autumn phenology in this forested peat bog. Specifically, we tested three competing hypotheses: first, that temperature is the dominant control on phenological events (hereafter referred to as H1). This hypothesis predicts that the observed phenological transition date is directly related to the degree of warming (Fig. 1 a). Second, that photoperiod is the dominant control on phenological events (hereafter referred to as H2). This hypothesis predicts that the observed phenological transition date is constant regardless of the degree of warming (Fig. 1 b). Third, that photoperiod constrains the phenological response to temperature (hereafter referred to as H3). This hypothesis predicts that the observed response to temperature is flat beyond a threshold temperature, t^* (Fig. 1 c).

We tracked phenological responses to the experimental treatments in two ways. Since August 2015 we have monitored the vegetation within each enclosure using digital repeat photography[6] (Fig. 1 d, e), and since April 2016 we have made weekly ground observations of vegetative and reproductive phenology on a variety of plant species.

For our analysis of camera imagery, we distinguished between three distinct vegetation types: an evergreen conifer, *Picea mariana* (black spruce); a deciduous conifer, *Larix laricina* (eastern tamarack or larch); and a mixed, ground-level shrub community dominated by *Rhododendron groenlandicum* (Labrador tea) and *Chamaedaphne calyculata* (leatherleaf). For each vegetation type, green-down—as determined by G_{CC}, a colour index derived from the digital images—in

[1]Department of Organismic and Evolutionary Biology, Harvard University, Cambridge, MA, USA. [2]School of Informatics, Computing and Cyber Systems, Northern Arizona University, Flagstaff, AZ, USA. [3]Center for Ecosystem Science and Society, Northern Arizona University, Flagstaff, AZ, USA. [4]Institute for the Study of Earth, Oceans and Space, University of New Hampshire, Durham, NH, USA. [5]Climate Change Science Institute and Environmental Sciences Division, Oak Ridge National Laboratory, Oak Ridge, TN, USA. *e-mail: Andrew.Richardson@nau.edu

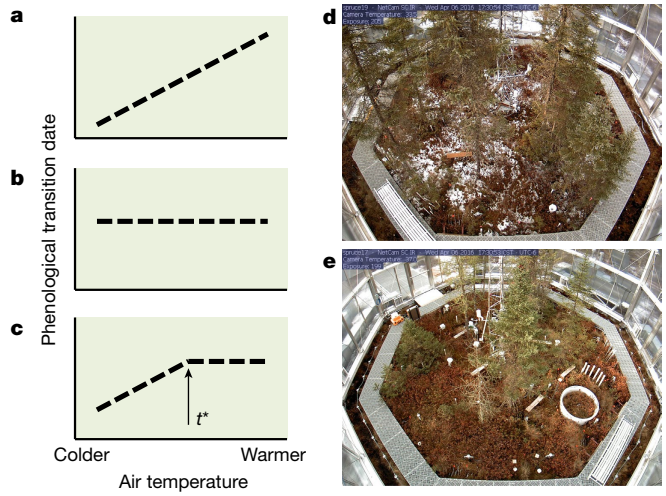

Fig. 1 | Testing competing hypotheses for phenological responses to warming using data from a whole-ecosystem warming experiment. **a**–**c**, Conceptual model of relationship between temperature and vegetation phenology, illustrating three competing hypotheses. **a**, Temperature is the dominant control (H1). **b**, Photoperiod is the dominant control (H2). **c**, Photoperiod limits the temperature response above the temperature threshold, t^* (H3). **d**, **e**, Sample digital camera imagery showing the inside of plot 19 (unheated control enclosure) (**d**) and plot 17 (+9.0 °C warming treatment enclosure) (**e**) on 6 April 2016. At the time the photographs were taken, the air temperature was 5 °C in plot 19 (note the last snow of the season), compared to 14 °C in plot 17.

autumn 2015 was delayed with increasing warming (Fig. 2a–c). The response to warming was significantly stronger (interaction effect between temperature and species, $P < 0.001$) for the mixed shrub community (about 5 days delay per 1 °C warming) than for either of the tree species (1–2 days delay per 1 °C warming), but was in all cases highly linear. Our results unequivocally support H1; that is, that temperature is the dominant control on the timing of autumn phenology. The fact that the temperature sensitivities were in all cases significantly different from zero allows us to reject H2. In no case did our breakpoint analysis (see Methods) identify a t^* value that substantially improved model fit (Extended Data Table 2), allowing us to reject H3. The above results are for autumn 2015, and comparable results were observed in autumn 2016 and 2017 (Supplementary Note 2).

Similarly, green-up in spring 2016 was advanced with increasing warming (Fig. 2d–f). The response to warming (1–2 days advancement per 1 °C warming) was not significantly different among vegetation types (interaction effect between temperature and species, $P = 0.34$). As in autumn, the fact that the temperature sensitivities were significantly different from zero allows us to reject H2. Breakpoint model analysis allowed us to reject H3, as in no case was a t^* value identified that would improve model fit (Extended Data Table 2). In spring, as in autumn, H1 is best supported by the experimental results. Results in spring 2017 were generally consistent with those for spring 2016 (Supplementary Note 2).

The above results clearly indicate a continued extension of the period of vegetation activity in response to future warming. By combining downscaled climate projections (Extended Data Fig. 2) from CMIP5[22] with the phenological temperature sensitivities estimated from Fig. 2 (Supplementary Note 3), we predict that the physiologically active season of the two conifer species may be extended by about a week under a 'CO_2 stabilization' climate scenario (representative concentration pathway (RCP)4.5, +2.9 ± 0.7 °C), and up to three weeks under a 'high CO_2 emission' scenario (RCP8.5, +5.9 ± 1.1 °C) by the year 2100 (Extended Data Table 3). Active season extension for the shrub layer is projected to be roughly twice as large as that of the conifers. These results are judged to be entirely plausible, given that future warming is not projected to exceed the levels of experimental warming at SPRUCE and that we are thus not extrapolating into unsampled climate space.

Previous work has shown that the seasonality of G_{CC} is a robust proxy for the seasonality of vegetation photosynthesis in both conifer forests and wetland ecosystems[23,24], and thus earlier plant green-up and delayed green-down at SPRUCE are almost certainly associated with a longer photosynthetically active period, and probably associated

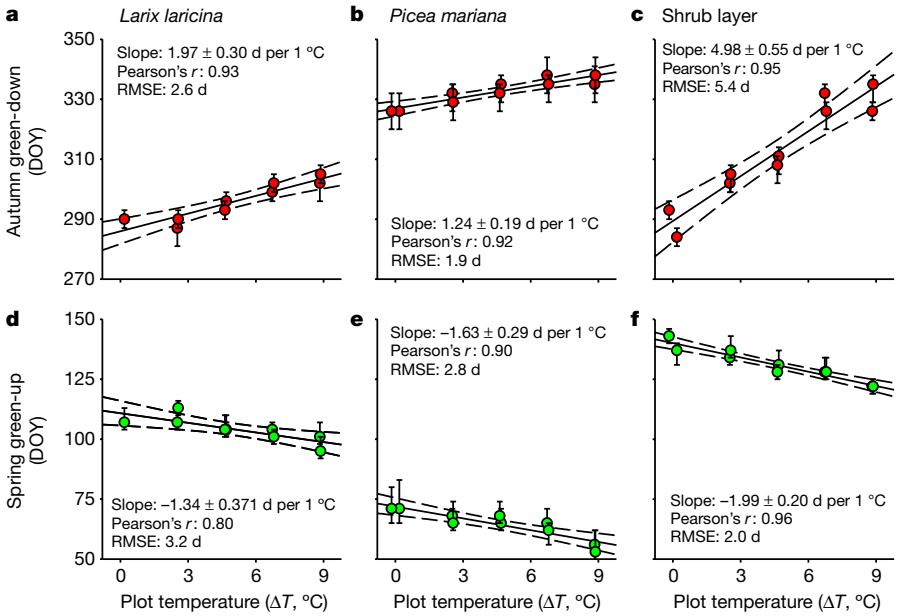

Fig. 2 | Effect of whole-ecosystem warming treatments on dates of autumn green-down and spring-green up, as derived from digital camera imagery. **a**–**f**, Response of autumn green-down (**a**–**c**, 2015) and spring green-up (**d**–**f**, 2016) phenology to experimental warming treatments for *L. laricina*, *P. mariana* and a mixed shrub layer community dominated by *R. groenlandicum* and *C. calyculata*, based on observations across $n = 10$ experimental enclosures ($n = 9$ for *Larix*, as in one enclosure this species was not within the camera field of view). Green-down and green-up are proxies for autumn senescence and spring onset, respectively. Error bars indicate 95% confidence interval around estimated phenological transition dates. Additional results are presented in Supplementary Note 2 and Extended Data Table 2. DOY, day of year; RMSE, root mean squared error.

Table 1 | Effect of SPRUCE warming treatments on spring and autumn phenological events (phenophases)

2016					2017			
Phenophase	*n*	*T* sensitivity	Breakpoints	*t**	*n*	*T* sensitivity	Breakpoints	*t**
Leaves growing	5	−3.19 ± 0.69	3	6.34 ± 1.08	7	−3.19 ± 1.25	5	5.46 ± 1.36
Shoots elongating	4	−3.53 ± 0.92	2	6.14 ± 1.59	5	−3.69 ± 1.04	4	7.12 ± 1.66
Flowering (cones open)	6	−2.51 ± 0.89	5	6.09 ± 1.89	7	−2.91 ± 1.33	5	6.74 ± 2.34
Flowers terminated					6	−1.45 ± 1.17	1	4.65
Fruiting	1	−2.56			6	−2.09 ± 1.38	3	6.06 ± 1.52
Autumn buds					3	−0.59 ± 1.03		
Autumn coloration (senescence)					6	2.70 ± 1.45	2	4.73 ± 2.88

Statistics (mean ± 1 s.d.) are calculated across all observed species. Sample size (*n*) indicates the number of species observed. '*T* sensitivity' is the temperature sensitivity, in days change per 1 °C warming, as estimated from the linear temperature model based on regression of transition date (*y*) on warming treatment (*x*). 'Breakpoints' indicates the number of species for which a *t** threshold was identified using the breakpoint temperature model (response is linear up to a temperature threshold *t**, and flat thereafter; see Fig. 1c and Methods). Species-level results are reported in Supplementary Note 5 and Extended Data Tables 4, 5.

with enhanced annual photosynthetic uptake (though not necessarily increased vegetation growth). This result is consistent with the analysis of long-term data from FLUXNET sites (http://fluxnet.fluxdata.org/, Supplementary Note 4, Extended Data Fig. 3), as well as previous experimental[19] and observational[25] studies. However, this does not necessarily indicate an increase in net carbon uptake or carbon sequestration under future warming, because the long-term carbon balance of this peatland forest ecosystem is probably dependent on the stability of the underlying peat deposits[26].

Camera-based results are generally consistent with direct observation of spring (2016 and 2017) and autumn (2017 only) phenological transitions for plant species spanning a range of leaf habits and growth forms (Table 1; see also Supplementary Note 5, Extended Data Tables 4, 5). Spring phenophases advanced by just over three days per 1 °C warming, providing strong support for H1. Autumn phenophases related to leaf coloration or senescence were delayed by almost three days per 1 °C warming, again providing support for H1. Relatively little variation was observed in dates of autumn bud set for *Chamaedaphne* and *Picea*, providing support for H2 for this particular phenophase of these species. Although *t** breakpoints that improved model fit were commonly identified, we note that in most cases the small-sample-corrected Akaike's information criterion (ΔAIC_C; see Methods) was greater than zero, which means that the simpler, linear temperature model was better supported by the data. Furthermore, the identified breakpoint temperatures were generally very high—below 4.5 °C in only a few instances—indicating that future warming would have to greatly exceed RCP4.5 projections before photoperiod constraints begin to limit phenological shifts. The ground observations therefore robustly support H1 over H2 or H3, and are consistent with the future extension of the active season at both ends.

There is abundant evidence in the literature that photoperiod has a role in triggering phenological events[27,28]. In many species, there has been a local adaptation of phenology to both photoperiod and temperature cues[5,15]. In some species and environments, photoperiod sets a hard limit on the phenological response to rising temperatures[4,15]. But, with warming of up to +9 °C above current levels, we found little evidence for this in most of the species and phenophases that we studied. Thus, photoperiod requirements are still being met even during the shortened winter simulated by the warmest enclosures. In the few cases in which there was evidence of a photoperiod effect, it was generally only a factor at temperatures well above current temperatures, again indicating that substantial future warming would be required for photoperiod to become limiting. These findings are consistent with a recent analysis showing that for high-latitude species, spring leaf-out was generally not sensitive to photoperiod[8].

The purported role of photoperiod as a phenological constraint is to prevent plants from responding to temperature signals at the 'wrong' time of the year[4]. However, if photoperiod is not a strong constraint on spring phenological development, then a counterintuitive prediction is that continued warming coupled with increasing frequency of climate extremes may increase the likelihood of spring frost damage[9,10]. At SPRUCE, atypical weather in March (unusually warm) and April (extreme cold) 2016 showed that in addition to triggering visually apparent phenological shifts, the warming treatments also advanced tissue de-hardening and thereby heightened the potential for spring frost damage (Supplementary Note 6, Extended Data Fig. 4). Following a spring frost event in which ambient temperatures dropped to −15 °C, we observed extensive foliar damage in the +9.0 °C enclosures (in which temperatures dropped to about −4 °C) and moderate damage in the +6.75 °C enclosures. Minimal damage occurred in the enclosures that received less warming and thus experienced colder minimum temperatures. This suggests that the transition from frost-hardy to frost-vulnerable is cued by warm temperatures[9], and is not constrained by photoperiod. Without photoperiod as a safety check on the de-hardening process, frost damage may be more severe and/or more frequent under future climate conditions. Woody plants generally have sufficient nonstructural carbon reserves to recover from occasional frost damage[10], but repeated damage could impair the competitive ability of susceptible species[9,29] (Extended Data Table 6).

Results from the first two-and-a-half years of the SPRUCE experiment, conducted in a winter-dormant ecosystem, show decisively that warming treatments directly influence vegetation phenology at both the start and end of the annual period of vegetation activity. These phenological shifts will almost certainly influence photosynthesis and transpiration[3,16], as well as feedbacks to the climate system through effects on the surface energy budget[12]. Future extension of the active season in most cases appears unlikely to be strongly constrained by photoperiod in this boreal ecosystem. Potentially inopportune responses to environmental signals may occur as the climate moves beyond the range of historical variability, as demonstrated by the spring frost damage in the warmest enclosures. Thus, temperature-tracking strategies evolved to guide phenological responses to historical year-to-year variation in weather may be increasingly mismatched to future conditions[5].

Online content

Any Methods, including any statements of data availability and Nature Research reporting summaries, along with any additional references and Source Data files, are available in the online version of the paper at https://doi.org/10.1038/s41586-018-0399-1.

Received: 15 August 2017; Accepted: 28 June 2018;
Published online 8 August 2018.

1. Settele, J. et al. in *Climate Change 2014: Impacts, Adaptation, and Vulnerability. Part A: Global and Sectoral Aspects. Contribution of Working Group II to the Fifth Assessment Report of the Intergovernmental Panel on Climate Change* (eds. Field, C. B. et al.) 271–359 (Cambridge Univ. Press, Cambridge, 2014).
2. Cleland, E. E., Chuine, I., Menzel, A., Mooney, H. A. & Schwartz, M. D. Shifting plant phenology in response to global change. *Trends Ecol. Evol.* **22**, 357–365 (2007).
3. Morisette, J. T. et al. Tracking the rhythm of the seasons in the face of global change: phenological research in the 21st century. *Front. Ecol. Environ.* **7**, 253–260 (2009).

4. Körner, C. & Basler, D. Phenology under global warming. *Science* **327**, 1461–1462 (2010).
5. Way, D. A. & Montgomery, R. A. Photoperiod constraints on tree phenology, performance and migration in a warming world. *Plant Cell Environ.* **38**, 1725–1736 (2015).
6. Sonnentag, O. et al. Digital repeat photography for phenological research in forest ecosystems. *Agric. For. Meteorol.* **152**, 159–177 (2012).
7. Hanson, P. J. et al. Attaining whole-ecosystem warming using air and deep-soil heating methods with an elevated CO_2 atmosphere. *Biogeosciences* **14**, 861–883 (2017).
8. Zohner, C. M., Benito, B. M., Svenning, J.-C. & Renner, S. S. Day length unlikely to constrain climate-driven shifts in leaf-out times of northern woody plants. *Nat. Clim. Change* **6**, 1120–1123 (2016).
9. Augspurger, C. K. Reconstructing patterns of temperature, phenology, and frost damage over 124 years: spring damage risk is increasing. *Ecology* **94**, 41–50 (2013).
10. Gu, L. et al. The 2007 Eastern US spring freeze: increased cold damage in a warming world. *Bioscience* **58**, 253–262 (2008).
11. Bonan, G. B. Forests and climate change: forcings, feedbacks, and the climate benefits of forests. *Science* **320**, 1444–1449 (2008).
12. Richardson, A. D. et al. Climate change, phenology, and phenological control of vegetation feedbacks to the climate system. *Agric. For. Meteorol.* **169**, 156–173 (2013).
13. Gill, A. L. et al. Changes in autumn senescence in northern hemisphere deciduous trees: a meta-analysis of autumn phenology studies. *Ann. Bot.* **116**, 875–888 (2015).
14. Laube, J. et al. Chilling outweighs photoperiod in preventing precocious spring development. *Glob. Change Biol.* **20**, 170–182 (2014).
15. Basler, D. & Körner, C. Photoperiod sensitivity of bud burst in 14 temperate forest tree species. *Agric. For. Meteorol.* **165**, 73–81 (2012).
16. Migliavacca, M. et al. On the uncertainty of phenological responses to climate change, and implications for a terrestrial biosphere model. *Biogeosciences* **9**, 2063–2083 (2012).
17. Slaney, M., Wallin, G., Medhurst, J. & Linder, S. Impact of elevated carbon dioxide concentration and temperature on bud burst and shoot growth of boreal Norway spruce. *Tree Physiol.* **27**, 301–312 (2007).
18. Gunderson, C. A. et al. Forest phenology and a warmer climate – growing season extension in relation to climatic provenance. *Glob. Change Biol.* **18**, 2008–2025 (2012).
19. Stinziano, J. R., Hüner, N. P. A. & Way, D. A. Warming delays autumn declines in photosynthetic capacity in a boreal conifer, Norway spruce (*Picea abies*). *Tree Physiol.* **35**, 1303–1313 (2015).
20. Vitasse, Y. & Basler, D. Is the use of cuttings a good proxy to explore phenological responses of temperate forests in warming and photoperiod experiments? *Tree Physiol.* **34**, 174–183 (2014).
21. Morin, X., Roy, J., Sonié, L. & Chuine, I. Changes in leaf phenology of three European oak species in response to experimental climate change. *New Phytol.* **186**, 900–910 (2010).
22. Brekke, L., Thrasher, B., Maurer, E. & Pruitt, T. *Downscaled CMIP3 and CMIP5 Climate Projections* (US Department of the Interior, Bureau of Reclamation, Technical Services Center, 2013).
23. Peichl, M., Sonnentag, O. & Nilsson, M. B. Bringing color into the picture: using digital repeat photography to investigate phenology controls of the carbon dioxide exchange in a boreal mire. *Ecosystems* **18**, 115–131 (2015).
24. Bowling, D. R. et al. Limitations to winter and spring photosynthesis of a Rocky Mountain subalpine forest. *Agric. For. Meteorol.* **252**, 241–255 (2018).
25. Richardson, A. D. et al. Influence of spring phenology on seasonal and annual carbon balance in two contrasting New England forests. *Tree Physiol.* **29**, 321–331 (2009).
26. Wilson, R. M. et al. Stability of peatland carbon to rising temperatures. *Nat. Commun.* **7**, 13723 (2016).
27. Singh, R. K., Svystun, T., AlDahmash, B., Jönsson, A. M. & Bhalerao, R. P. Photoperiod- and temperature-mediated control of phenology in trees – a molecular perspective. *New Phytol.* **213**, 511–524 (2017).
28. Zohner, C. M. & Renner, S. S. Perception of photoperiod in individual buds of mature trees regulates leaf-out. *New Phytol.* **208**, 1023–1030 (2015).
29. Hufkens, K. et al. Ecological impacts of a widespread frost event following early spring leaf-out. *Glob. Change Biol.* **18**, 2365–2377 (2012).

Acknowledgements This material is based upon work supported by the US Department of Energy (DOE), Office of Science, Office of Biological and Environmental Research. Oak Ridge National Laboratory is managed by UT-Battelle, LLC, for DOE under contract DE-AC05-00OR22725. Support for PhenoCam has come from the National Science Foundation (EF-1065029, EF-1702697). D. Hollinger, M. Carbone and C. Iverson provided feedback on a draft manuscript. E. Ward assisted with litter collection. For CMIP, we acknowledge the World Climate Research Programme's Working Group on Coupled Modelling. We thank the climate modelling groups (listed in Supplementary Note 3) for making their model output available. DOE's Program for Climate Model Diagnosis and Intercomparison additionally provides coordinating support and led development of software infrastructure for CMIP in partnership with the Global Organization for Earth System Science Portals.

Reviewer information *Nature* thanks M. Tjoelker and the other anonymous reviewer(s) for their contribution to the peer review of this work.

Author contributions A.D.R. designed the study with input from P.J.H. A.D.R., K.H., D.M.A., T.M., M.E.F., B.S. and M.B.K. contributed PhenoCam imagery and derived data. J.M.L., W.R.N., J.M.W. and R.R.H. contributed phenological observations. J.M.W. contributed data on frost damage. M.B.K., W.R.N. and P.J.H. maintained site infrastructure including warming treatments and meteorological observations. A.D.R. assembled datasets and conducted the analysis. A.D.R. drafted the manuscript. All authors commented on and approved the final manuscript.

Competing interests The authors declare no competing interests.

Additional information

Extended data is available for this paper at https://doi.org/10.1038/s41586-018-0399-1.
Supplementary information is available for this paper at https://doi.org/10.1038/s41586-018-0399-1.
Reprints and permissions information is available at http://www.nature.com/reprints.
Correspondence and requests for materials should be addressed to A.D.R.

METHODS

Statistical methods were not used to predetermine sample size for the regression design. The warming treatments were randomized among 10 plots with similar vegetation and uniform peat depths. Investigators were not blinded to allocation during experiments and outcome assessment.

Study site and experimental design. The SPRUCE experiment is located within the S1 peat bog at the Marcell Experimental Forest (47° 30.171′ N, 93° 28.970′ W)[30], approximately 40 km north of Grand Rapids in north-central Minnesota. The historical climate at the site is sub-humid continental: mean annual temperature is 4 °C, mean annual precipitation is 750 mm, and extreme temperatures range from −38 °C to +30 °C. Because this ecosystem is located at the southern edge of the boreal zone, it is considered particularly vulnerable to climate change.

The S1 bog is an ombotrophic peatland with a perched water table. Trees are approximately 5–8 m in height. Canopy vegetation is dominated by the tree species *P. mariana* (Mill.) B.S.P. (black spruce), with additional contributions from *L. laricina* (Du Roi) K. Koch (eastern tamarack or larch). *P. mariana* and *L. laricina* both have a vast geographic range across North America, from Alaska east to Quebec and Labrador, and south to the Great Lakes and New England. A number of closely related *Picea* and *Larix* species are distributed across the boreal zone of northern Europe, Scandinavia and much of Russia and Siberia, indicating the relevance of results of this experiment to our understanding of boreal ecosystem processes globally.

The SPRUCE understory is dominated by the evergreen shrubs *R. groenlandicum* (Oeder) Kron and Judd (Labrador tea) and *C. calyculata* (L.) Moench. (leatherleaf), and is underlain by a bryophyte layer dominated by *Sphagnum* spp. moss. Other common plant species include the evergreen shrub *Kalmia polifolia* Wangenh. (bog laurel), the deciduous shrub *Vaccinium angustifolium* Aiton 1789 not Benth. 1840 (lowbush blueberry), the sedge *Eriophorum* spp. (cottongrass), and the perennial herb *Maianthemum trifolium* (L.) Sloboda (false Solomon's seal).

At SPRUCE, experimental temperature (+0 °C 'unheated control' to +9.0 °C, in 2.25 °C increments for both air and deep soil) and CO_2 (ambient and elevated, approximately 400 and 900 p.p.m., respectively) treatments are being applied through the use of large (approximately 12-m wide, 8-m high) open-topped octagonal enclosures[7]. Overall, five temperature treatments are paired with two CO_2 treatments, yielding a total of ten enclosures (additionally, there are two 'ambient environment' plots without constructed enclosures). Each enclosure is hydrologically isolated from the rest of the bog by a sheet pile corral which has been driven 3–4 m through the peat into the underlying ancient lake sediments. Outflow pipes allow for lateral drainage from each enclosure. Within each enclosure, warming of the deep soil began in June 2014, while aboveground warming was initiated in August 2015 and at this time the phenological observations were commenced in each individual plot (note that pre-treatment observations were made in a common area, outside of the enclosures, beginning in 2010). CO_2 treatments were switched on in June 2016.

For context, the warmest enclosures (+9.0 °C) simulate current climate conditions of Wichita, Kansas (mean annual temperature 13 °C, mean annual precipitation 850 mm), located approximately 1,100 km (10° of latitude) to the south. The SPRUCE experiment, with treatments that will exceed the historical range of climatic variability (Extended Data Fig. 1), is intentionally planned to push the system past projected warming levels to approach or include tipping points for any number of ecosystem response variables. The regression-based experimental design facilitates the estimation of temperature response functions, which may be nonlinear[7].

The enclosure design, and detailed performance metrics for the above- and belowground warming, along with a discussion of potential artefacts, are more fully described and assessed in a previous publication[7]. Observed temperature differentials were consistent with the nominal warming treatments for target enclosures. Warming was homogeneous within individual enclosures, and was sustained over time (see Supplementary Note 1, Extended Data Table 1).

Phenological observations. We are using two methods to track the phenological responses of vegetation to warming and elevated CO_2 in each enclosure. First, beginning in August 2015, we installed digital cameras[31], or phenocams[32], in each enclosure to track seasonal variation in vegetation 'greenness', a proxy for vegetation phenology and associated physiological activity[6,33–35]. Second, beginning in April 2016, human observers have been directly tracking phenological events of both woody and herbaceous species.

PhenoCam imagery. Digital cameras (NetCam model SD130BN, StarDot Technologies) were configured and installed following standard protocols of the PhenoCam network[36]. Cameras record sequential visible-light (red, green, blue; RGB) and visible + infrared images[37] every 30 min from 4:00 to 22:00, every day of the year. Minimally compressed JPEG images, accompanied by a metadata file containing the current status of all camera settings and diagnostics, are uploaded via file transfer protocol to the PhenoCam server for archiving and processing; a local copy is also maintained on a server running at SPRUCE. The filename of every image identifies the enclosure in which the picture was recorded, as well as a date and time stamp in local standard time.

The aluminium structural members of each enclosure provided convenient and consistent mounting points for the cameras. All cameras were mounted, at a height of 6 m, in the middle of the third horizontal structural member on the south wall of each enclosure. Cameras were enclosed in lightweight, compact weatherproof enclosures (model ENC-OUTD3, StarDot Technologies). Network connectivity and DC power were delivered to each camera using a single Ethernet cable and standard power-over-Ethernet technology. To reduce the likelihood of lightning damage, an Ethernet surge protector (ProtectNet model PNET1GB, APC by Schneider Electric) was installed on the camera end of each Ethernet cable, and grounded to the mounting point.

All imagery is posted in near-real time to the PhenoCam project web page (http://phenocam.sr.unh.edu/), where it is publicly available. Images are processed nightly, using standard PhenoCam routines[6,36]. In brief, this consists of several steps. First, we defined three separate regions of interest (ROIs) for each camera field of view, demarcating (1) *Picea* trees; (2) *Larix* trees; and (3) the mixed shrub layer. The ROI definitions are converted to binary masks, so that image analysis can be completed separately for each vegetation type. Next, images were read in sequentially, and for each vegetation type the mean pixel value for each of the three colour channels (red, green and blue; for the purposes of the present analysis we used only the visible-wavelength imagery) was calculated across the corresponding ROI, yielding a digital number (DN) triplet (R_{DN}, G_{DN}, B_{DN}). Then for each ROI in each image, we calculated the green chromatic coordinate G_{CC}, which has previously been shown to be a reliable metric for characterizing the seasonal trajectory of vegetation colour and activity[6,31,38]:

$$G_{CC} = \frac{G_{DN}}{R_{DN} + G_{DN} + B_{DN}}$$

Basic quality control included eliminating images that were recorded when the sun was less than 5° above the horizon, images that were too dark or images that were too bright. Additionally, because snow might obscure the vegetation of interest, for each day from late August 2015 through the end of December 2017, we visually inspected the mid-day image from each camera. We flagged images in which there was (1) snow on the ground; or (2) snow on trees. We excluded from further processing all days on which the camera's view of the vegetation of interest was potentially contaminated by snow. For the shrub layer, this meant eliminating images from days with snow on the ground; for *Picea* and *Larix*, this meant eliminating images from days with snow on trees. The frequency of snow decreased with increasing plot temperature, from over 100 days per year with snow on the ground in the unheated enclosures (from late October to early May), to less than 30 days per year in the +9.0 °C enclosures (from late November to early February). The longest period of continuous snow cover was almost three months in the unheated enclosures, compared with only two weeks in the +9.0 °C enclosures.

Next, we determined 3-day G_{CC} values using the 90th quantile method[6]. We then used a spline-based method to sequentially remove outliers in three iterative steps. Finally, we re-fit the spline, and used the summertime maxima and dormant-season minima to define the seasonal G_{CC} amplitude, from which we were then able to identify dates at which 10%, 25% and 50% of the seasonal amplitude were reached in autumn (senescent or green-down phase) and spring (onset or green-up phase). Uncertainties on these dates were then derived based on the uncertainty around the smoothing spline. Our analysis here focuses on the 25% amplitude threshold dates.

Ground observations. Ground observations of spring phenology were made at approximately weekly intervals by W.R.N. and J.M.L. in 2016, and by R.R.H. in 2017. The protocol used by W.R.N. and R.R.H. involved recording, on a preprinted form for each of the 10 enclosures and the two ambient environment plots, whether or not ('yes' or 'no') specific vegetative and reproductive phenophases were observed each week. Observations were conducted on a selection of woody species (the trees *Picea* and *Larix*; the evergreen shrubs leatherleaf, bog laurel, Labrador tea and lowbush blueberry), as well as a sedge (cottongrass) and a perennial herb (false Solomon's seal). We transcribed the data by taking as the observed date the first survey date on which an event was definitively observed (that is, 'no' through week 4, followed by 'yes' in week 5: the event occurred in week 5). Not all phenophases were observed for all species, and in some difficult-to-observe cases, the data were deemed not reliable because of some inconsistencies in the recorded data (for example, blank cells rather than 'no', or 'no' followed by 'yes' followed by 'no' again) or poor representation of the species in question in some of the plots (for example, bog laurel and lowbush blueberry are sparsely distributed). All transcribed data of questionable reliability were excluded from the analysis.

J.M.L.'s protocol involved recording the first date at which *Larix* leaf buds were observed to be just beginning to break (data recorded for all ten enclosures,

plus the two ambient environment plots), and the first date on which flowers of leatherleaf, bog laurel and Labrador tea were observed in each enclosure (data recorded in only half of the treated enclosures, plus one or both of the ambient environment plots). Although data recorded by J.M.L. are not as complete as those recorded by W.R.N., they are included to demonstrate the robustness of the observed patterns.

On-site meteorological data. Air temperature and relative humidity were measured (model HMP-155, Vaisala) at four points above the peat surface within each enclosure (0.5, 1, 2 and 4 m), and 30-min mean values recorded. We used the measured air temperature at 2 m in our analyses. SPRUCE environmental data[39] are available through the Vista Data Vision portal (http://sprucedata.ornl.gov).

Historical perspective and future climate projections. To put the weather during winter and spring of 2016 in historical context (122 year record), we used data from the National Climatic Data Center of the NOAA. Specifically, we used summary data from the State of the Climate report (https://www.ncdc.noaa.gov/sotc/national/), and three-month divisional temperature rankings (https://www.ncdc.noaa.gov/temp-and-precip/climatological-rankings/). The SPRUCE site falls within Minnesota's climate division 2.

To place our results in the context of projected warming trends over the coming century, we used downscaled (1/8°) climate projections from a selection of ten models (see Supplementary Note 2) contributing to the CMIP5 multimodel ensemble dataset[22,40]. We used output for two RCP scenarios: RCP4.5 (CO_2 stabilization) and RCP8.5 (high CO_2 emission)[41,42]. To quantify future trends, we calculated the projected decadal mean air temperature change relative to the 2006–2015 mean for each model.

Statistical analysis. To characterize the relationship between air temperature and phenological timing (H1 and H2), we used ordinary linear regression, with the observed phenological date as the dependent variable, y_i, and the measured air temperature differential for each plot (see Supplementary Note 1) as the independent variable, x_i. The regression slope β thus gives the temperature sensitivity in days per 1 °C warming for the 'linear temperature model'. To account for potential effects of elevated CO_2 on phenology, we also analysed data (where appropriate) using a 'linear temperature and CO_2 model', which included temperature, CO_2 (elevated and ambient) and a temperature × CO_2 interaction effect. All tests were two-sided, at a significance level of 0.05.

For breakpoint analysis (H3), we fit a three-parameter (α, β and t^*) 'breakpoint temperature model', which was specified as:

$$y_i = \alpha + \beta x_i + \epsilon_i \text{ for } x_i < t^*$$

and

$$y_i = \alpha + \beta t^* + \epsilon_i \text{ for } x_i \geq t^*$$

in which x_i and y_i are as for the ordinary linear regression, ϵ_i is the regression residual and t^* is the temperature breakpoint, as illustrated in Fig. 1. We constrained t^* to fall in the range of 2–9 °C. An edge-hitting value of $t^* = 9$ °C was obtained when the linear model fit the data every bit as well as the breakpoint model.

We used AIC[43] to identify whether the linear model or the breakpoint model was best supported by the available data. AIC is typically calculated as:

$$\text{AIC} = n\log\sigma^2 + 2p$$

in which n is the number of observations, p is the number of fit parameters plus one, and σ^2 is the residual sum of squares divided by n. When n is small relative to p, the small-sample-corrected criterion, AIC_C, is preferred[43]:

$$\text{AIC}_C = \text{AIC} + \frac{2p(p+1)}{n-p-1}$$

AIC effectively balances improving explanatory power (lower σ^2) against increasing complexity (larger p), and thus AIC selects against over-parameterized models. The model with the lowest AIC is considered the best model given the data, and the absolute difference in AIC_C scores between two models can be used to evaluate the weight of evidence in support of the better model. If the difference (ΔAIC) is small or zero then the two models are equally good. But, if $\Delta\text{AIC} \approx 2.0$, then the model with the lower AIC_C is almost three times more likely to be the best[43].

Reporting summary. Further information on experimental design is available in the Nature Research Reporting Summary linked to this paper.

Data availability. PhenoCam imagery is publicly available through the project web page (http://phenocam.sr.unh.edu), and the phenological datasets used in this study are available through the SPRUCE data portal[44,45].

30. Kolka, R., Sebestyen, S., Verry, E. S. & Brooks, K. *Peatland Biogeochemistry and Watershed Hydrology at the Marcell Experimental Forest* (CRC, Boca Raton, 2011).
31. Richardson, A. D. et al. Use of digital webcam images to track spring green-up in a deciduous broadleaf forest. *Oecologia* **152**, 323–334 (2007).
32. Brown, T. B. et al. Using phenocams to monitor our changing Earth: toward a global phenocam network. *Front. Ecol. Environ.* **14**, 84–93 (2016).
33. Keenan, T. F. et al. Tracking forest phenology and seasonal physiology using digital repeat photography: a critical assessment. *Ecol. Appl.* **24**, 1478–1489 (2014).
34. Richardson, A. D., Klosterman, S. & Toomey, M. in *Phenology: An Integrative Environmental Science* (ed. Schwartz, M. D.) 413–430 (Springer, Dordrecht, 2013).
35. Toomey, M. et al. Greenness indices from digital cameras predict the timing and seasonal dynamics of canopy-scale photosynthesis. *Ecol. Appl.* **25**, 99–115 (2015).
36. Richardson, A. D. et al. Tracking vegetation phenology across diverse North American biomes using PhenoCam imagery. *Sci. Data* **5**, 180028 (2018).
37. Petach, A. R., Toomey, M., Aubrecht, D. M. & Richardson, A. D. Monitoring vegetation phenology using an infrared-enabled security camera. *Agric. For. Meteorol.* **195–196**, 143–151 (2014).
38. Richardson, A. D., Braswell, B. H., Hollinger, D. Y., Jenkins, J. P. & Ollinger, S. V. Near-surface remote sensing of spatial and temporal variation in canopy phenology. *Ecol. Appl.* **19**, 1417–1428 (2009).
39. Hanson, P., Riggs, J., Nettles, W., Krassovski, M. & Hook, L. *SPRUCE Whole Ecosystems Warming (WEW) Environmental Data Beginning August 2015* https://doi.org/10.3334/CDIAC/spruce.032 (2016).
40. Maurer, E. P., Brekke, L., Pruitt, T. & Duffy, P. B. Fine-resolution climate projections enhance regional climate change impact studies. *Eos* **88**, 504 (2007).
41. Riahi, K. et al. RCP 8.5—a scenario of comparatively high greenhouse gas emissions. *Clim. Change* **109**, 33–57 (2011).
42. Thomson, A. M. et al. RCP4.5: a pathway for stabilization of radiative forcing by 2100. *Clim. Change* **109**, 77–94 (2011).
43. Burnham, K. P. & Anderson, D. R. *Model Selection and Multimodel Inference: a Practical Information–Theoretic Approach* (Springer, New York, 2002).
44. Richardson, A. D. et al. *SPRUCE Ground Observations of Phenology in Experimental Plots 2016–2017* https://doi.org/10.3334/CDIAC/spruce.044 (2018).
45. Richardson, A. D. et al. *SPRUCE Vegetation Phenology in Experimental Plots from Phenocam Imagery 2015–2017* https://doi.org/10.3334/CDIAC/spruce.045 (2018).

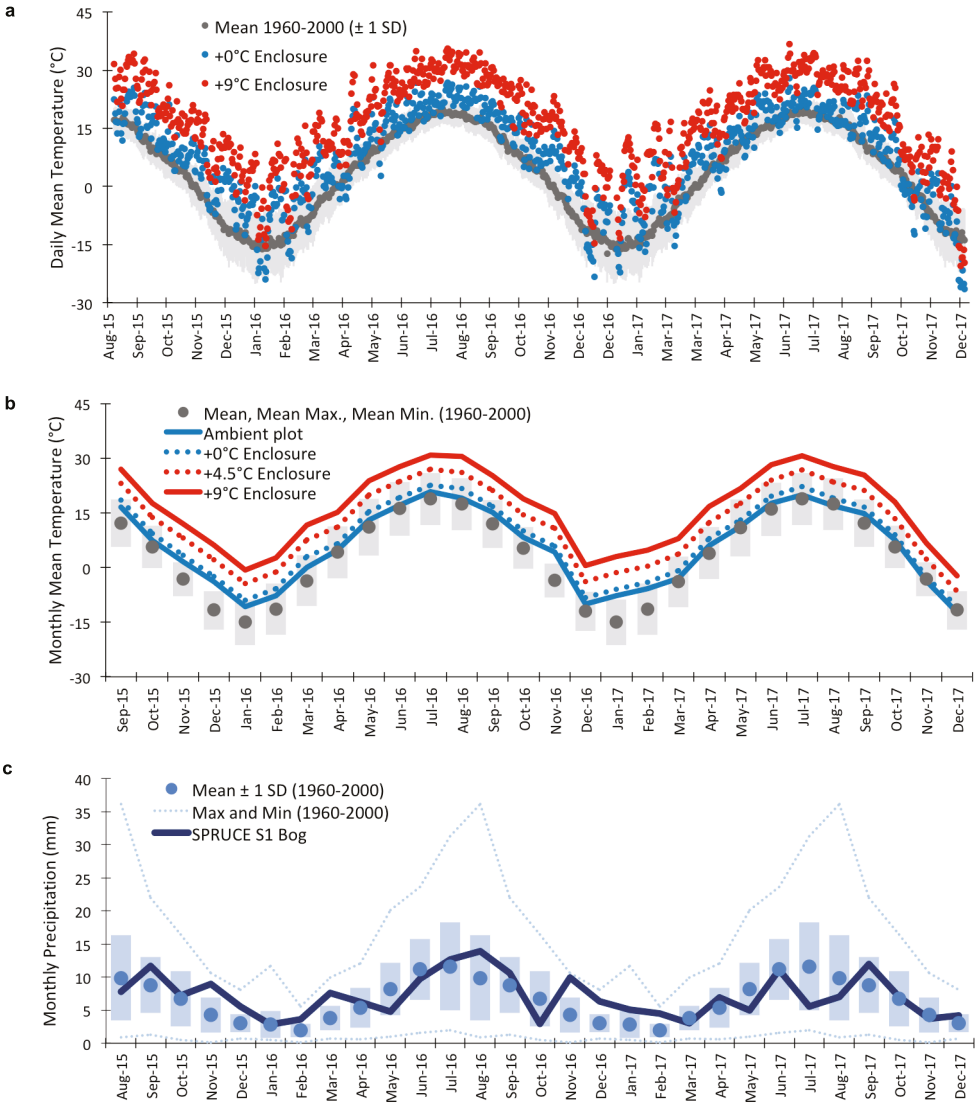

Extended Data Fig. 1 | Air temperature and precipitation in the SPRUCE S1 bog (August 2015 to December 2017) relative to long-term (1960–2000) means and variability. a, Long-term daily mean temperature (°C, ± 1 s.d. indicated by shading), compared with daily mean temperature (calculated from 30-min means, based on $n = 2$ sensors mounted at 2-m height in each enclosure) in a +0 °C enclosure (unheated control) and a +9.0 °C enclosure. **b**, Long-term monthly mean temperature (mean daily maximum and mean daily minimum indicated by shaded bars), compared with monthly mean temperature (calculated from daily means, as in **a**) in different experimental treatments. **c**, Long-term monthly mean precipitation (mm, ± 1 s.d. indicated by shading, with maxima and minima indicated by dotted lines), compared with measured monthly precipitation ($n = 1$ rain gauge) in the S1 bog.

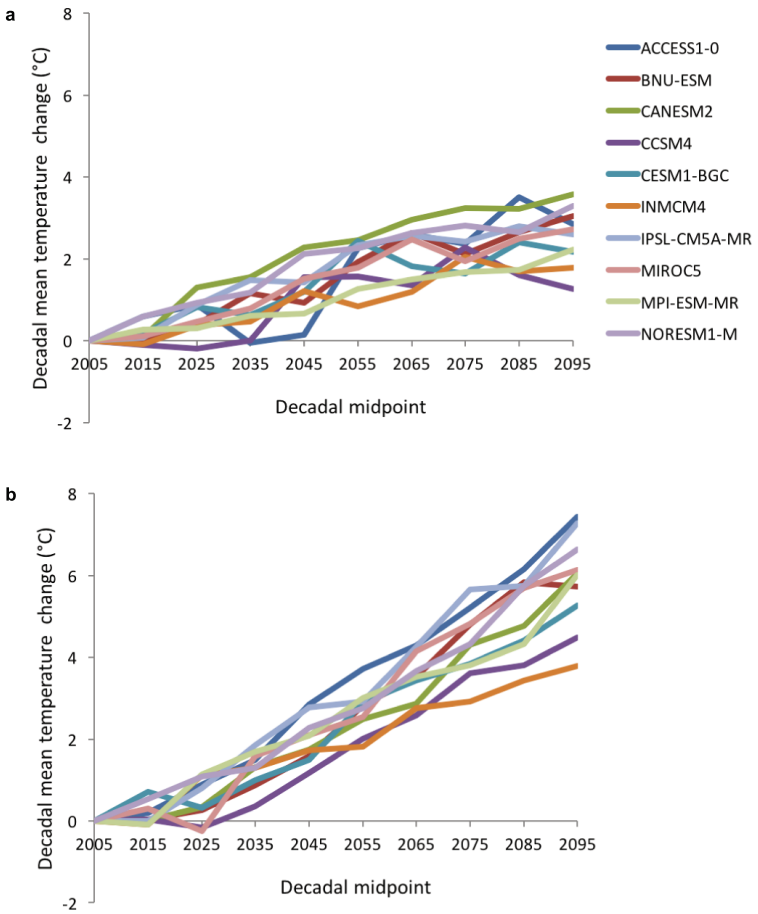

Extended Data Fig. 2 | Decadal mean temperature change (relative to 2006–2015 mean) projections from ten CMIP5 earth system models for the SPRUCE site. a, Stabilization climate scenario (RCP4.5). **b**, High emission climate scenario (RCP8.5).

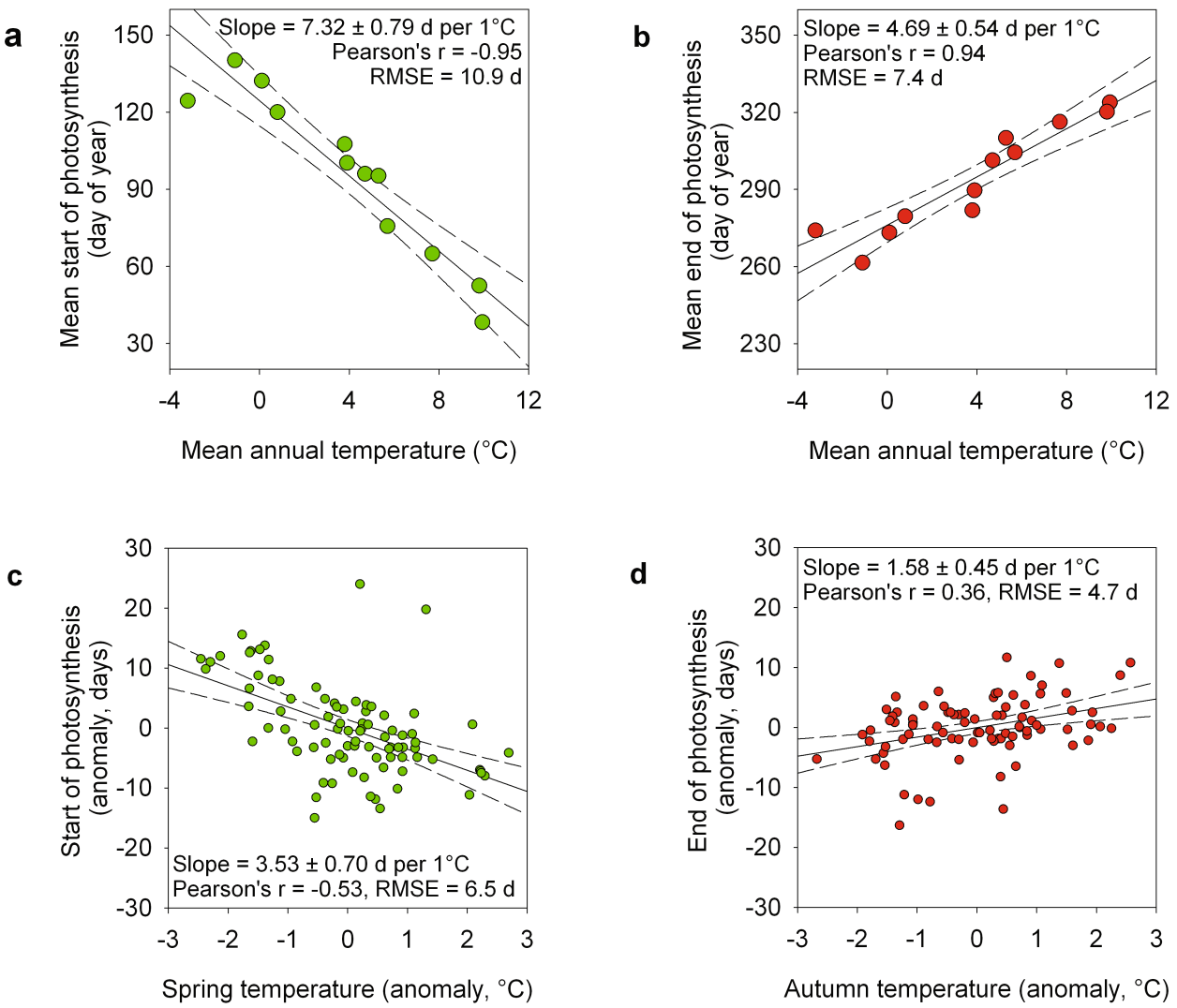

Extended Data Fig. 3 | Relationships between air temperature and the start and end of the photosynthetic uptake period, as derived from FLUXNET data for evergreen conifer-dominated sites. a–d, Across-site patterns in spring (**a**) and autumn (**b**) in relation to mean annual temperature ($n = 12$ sites), and within-sites patterns in spring (**c**) and autumn (**d**) in relation to seasonal temperature anomalies ($n = 86$ site-years).

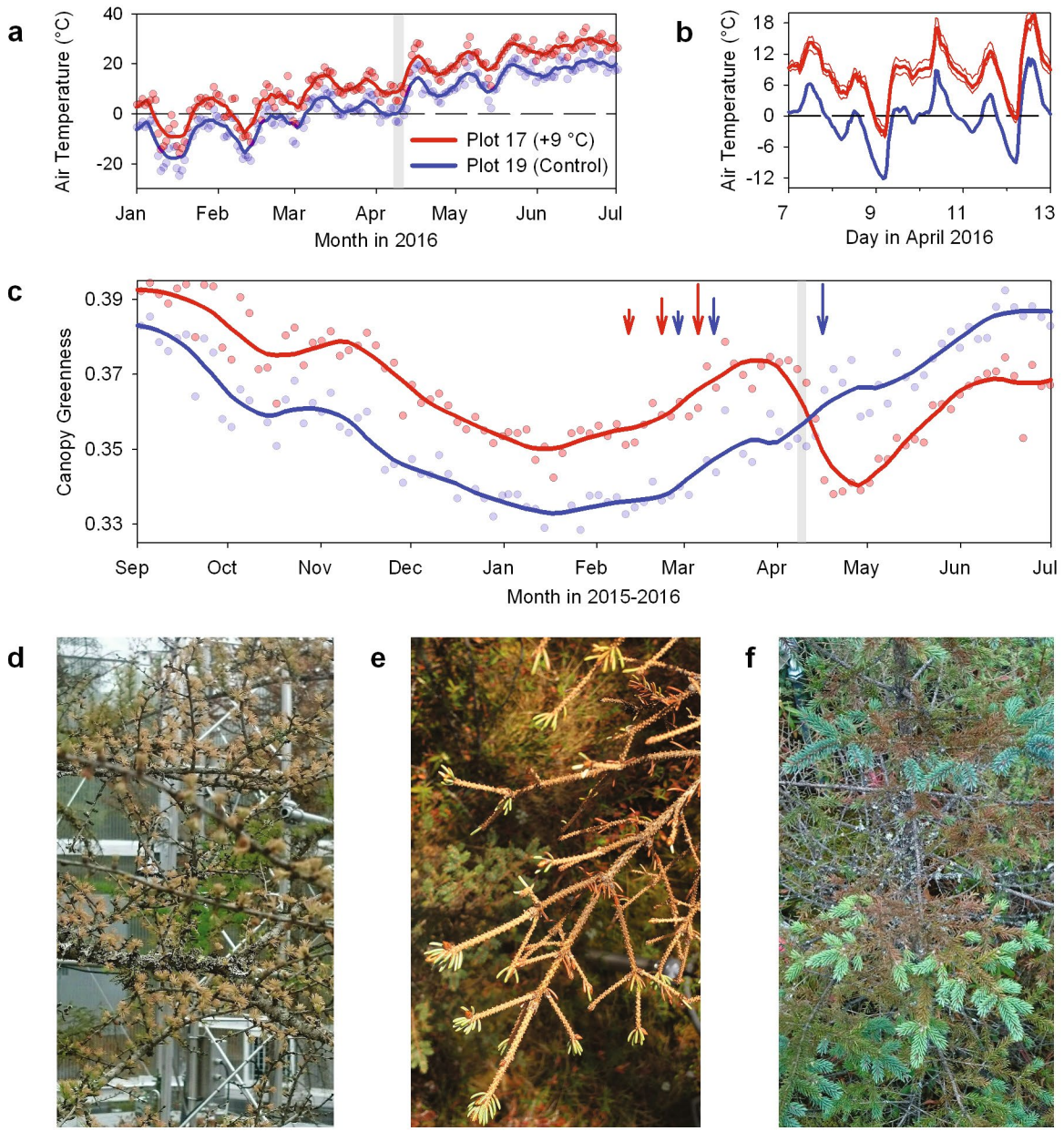

Extended Data Fig. 4 | Unusually warm weather in late winter, followed by extreme cold in early April, resulted in severe frost damage in the warmest enclosures at SPRUCE in 2016. a, Time series of daily mean air temperature, comparing plot 17 (+9.0 °C warming) and plot 19 (unheated enclosure), during the winter and spring of 2016. By the time the frost event occurred (grey shading), the daily mean temperature in plot 17 had been above freezing for over a month, but had repeatedly dropped below freezing in plot 19. **b**, Time series of 30-min air temperature—again comparing plot 17 and plot 19—leading up to and immediately following the frost event, which occurred on the morning of 9 April and again on 12 April. The thin red lines indicate the variability (maximum and minimum) across $n = 5$ temperature sensors in plot 17. **c**, Time series of daily G_{CC}, the green chromatic coordinate, for *Picea* trees in plot 17 and plot 19. Arrows denote spring green-up dates (progressively larger arrows corresponding to 10%, 25% and 50% of seasonal amplitude) estimated from G_{CC}. The pronounced decline in G_{CC} in plot 17 following the frost event (grey shading) is readily apparent. Trees in plot 19 retained sufficient frost hardiness that they were undamaged, despite experiencing much colder temperatures. **d**, Brown frost-damaged *Larix* foliage in plot 17. **e**, *Picea* branches in plot 17, showing loss of most foliage from previous years, with green foliage from the 2015 flush retained only at branch tips. **f**, *Picea* branches with frost-damaged foliage from previous years, but healthy green foliage from the 2016 flush.

Extended Data Table 1 | Mean daily air temperature and temperature differentials associated with whole-ecosystem warming

Plot number	Plot 21	Plot 07	Plot 19	Plot 06	Plot 11	Plot 20	Plot 13	Plot 04	Plot 08	Plot 16	Plot 10	Plot 17
Nominal Treatment	Ambient	Ambient	Unheated	Unheated	+2.25	+2.25	+4.5	+4.5	+6.75	+6.75	+9.0	+9.0
Mean daily mean temperature (°C)												
Aug-Dec 2015	7.0	6.8	8.2	8.6	10.8	10.9	12.9	13.1	15.2	15.3	17.1	17.2
Jan-Jun 2016	2.9	2.9	4.5	4.9	7.2	7.4	9.5	9.4	11.4	11.4	13.4	13.5
Jul-Dec 2016	9.6	9.7	11.1	11.4	13.8	13.8	15.9	15.9	17.9	18.0	20.1	20.2
Jan-Jun 2017	2.8	3.0	4.5	4.8	7.3	7.2	9.3	9.4	11.5	11.5	13.6	13.6
Jul-Dec 2017	9.8	9.8	11.3	11.5	13.9	13.9	15.9	16.0	18.0	18.2	20.3	20.3
Mean temperature differential (ΔT, °C)												
Aug-Dec 2015	-1.4	-1.6	-0.2	0.2	2.4	2.5	4.5	4.7	6.8	6.9	8.7	8.8
Jan-Jun 2016	-1.8	-1.8	-0.2	0.2	2.5	2.7	4.7	4.7	6.6	6.6	8.7	8.8
Jul-Dec 2016	-1.6	-1.5	-0.2	0.2	2.5	2.5	4.6	4.6	6.6	6.8	8.9	8.9
Jan-Jun 2017	-1.8	-1.7	-0.2	0.2	2.6	2.5	4.7	4.7	6.9	6.9	8.9	8.9
Jul-Dec 2017	-1.6	-1.6	-0.1	0.1	2.6	2.5	4.6	4.6	6.7	6.8	9.0	9.0
Mean ΔT ± 1 SD	-1.6 ± 0.2	-1.6 ± 0.1	-0.2 ± 0.0	0.2 ± 0.0	2.5 ± 0.1	2.6 ± 0.1	4.6 ± 0.1	4.7 ± 0.1	6.7 ± 0.1	6.8 ± 0.1	8.8 ± 0.1	8.9 ± 0.1

Daily means are calculated on the basis of the mean half-hour data for two temperature sensors mounted at 2-m height. Temperature differentials (ΔT) are calculated relative to the mean of the two unheated enclosures (plots 19 and 6). Plots are arranged in order of increasing ΔT; overall mean $\pm$ 1 standard deviation (SD). ΔT is calculated across $n = 5$ multi-month means.

Extended Data Table 2 | Effect of SPRUCE warming treatments on spring green-up and autumn green-down

			Linear Temperature Model				Breakpoint Temperature Model			
Species	Phenophase	Mean DOY	Pearson *r*	RMSE	Slope ± 1 SE	T effect	RMSE	Slope ± 1 SE	t^* ± SE	ΔAICc
Larix laricina	Autumn 2015	296 ± 6	0.93	2.6	1.97 ± 0.30	P < 0.001	-	-	-	-
	Spring 2016	104 ± 5	-0.80	3.2	-1.34 ± 0.37	P < 0.01	-	-	-	-
	Autumn 2016	298 ± 10	0.64	8.1	2.12 ± 0.95	P = 0.06	-	-	-	-
	Spring 2017	101 ± 4	-0.81	2.6	-1.11 ± 0.30	P < 0.01	2.5	-3.15 ± 1.27	3.50 ± 0.90	+5.1
	Autumn 2017	293 ± 11	0.66	9.0	2.48 ± 1.07	P = 0.05	-	-	-	-
Picea marinana	Autumn 2015	333 ± 4	0.92	1.9	1.24 ± 0.19	P < 0.001	1.6	1.61 ± 0.35	6.43 ± 1.08	+1.6
	Spring 2016	64 ± 6	-0.90	2.8	-1.63 ± 0.29	P < 0.001	-	-	-	-
	Autumn 2016	325 ± 9	0.86	5.1	2.47 ± 0.52	P < 0.01	5.3	2.82 ± 0.74	7.48 ± 1.81	+5.4
	Spring 2017	88 ± 12	0.19	12.2	0.69 ± 1.25	P = 0.60	-	-	-	-
	Autumn 2017	315 ± 7	0.91	3.2	2.00 ± 0.33	P < 0.001	3.1	2.42 ± 0.43	6.90 ± 1.17	+3.5
Shrub layer	Autumn 2015	312 ± 17	0.95	5.4	4.98 ± 0.55	P < 0.0001	5.3	5.64 ± 0.74	7.55 ± 0.91	+4.0
	Spring 2016	131 ± 7	-0.96	2.0	-1.99 ± 0.20	P < 0.0001	-	-	-	-
	Autumn 2016	313 ± 19	0.92	7.5	5.25 ± 0.77	P < 0.001	7.4	6.08 ± 1.04	7.31 ± 1.16	+4.2
	Spring 2017	128 ± 7	-0.67	5.8	-1.48 ± 0.59	P = 0.04	-	-	-	-
	Autumn 2017	305 ± 13	0.94	4.8	3.66 ± 0.49	P < 0.0001	3.4	5.49 ± 0.73	5.59 ± 0.58	-2.0

Results (derived from PhenoCam imagery) are shown from the start of the whole-ecosystem warming experiment (autumn 2015), on the basis of observations across $n = 10$ experimental enclosures ($n = 9$ for *Larix*, as in one enclosure this species was not within the camera field of view). Mean transition dates are reported ± 1 s.d. Statistics for the linear temperature model are based on regression of transition date (y) on warming treatment (x), and the model slope is the phenological temperature sensitivity in days per 1 °C warming. The '*T* effect' column reports the *P* value for the null hypothesis of no temperature effect. Statistics for the breakpoint temperature model are based on a model in which the response to warming treatment is assumed to be linear up to a temperature threshold t^*, and flat thereafter (see Methods for additional details). No statistics are reported for cases in which a t^* could not be identified or where the addition of t^* did not improve model fit. ΔAIC_C is the difference in AIC (corrected for small sample sizes) between the linear temperature model and the breakpoint temperature model, with a positive value indicating that the linear temperature model is better supported by the data and a negative value indicating that the beakpoint temperature model is better supported by the data. RMSE, root mean squared error. SE, standard error. Results not shown for the linear temperature and CO_2 model as the CO_2 effect and $CO_2 \times T$ interaction effect were generally not significant (see Supplementary Note 2 for additional information).

Extended Data Table 3 | Projected future extension of the period of vegetation activity

Temperature sensitivity (days per 1°C warming)		*Larix laricina*	*Picea mariana*	Shrub layer
Onset of green-up		-1.3 ± 0.4	-1.6 ± 0.3	-2.0 ± 0.2
Completion of green-down		2.0 ± 0.3	1.2 ± 0.2	5.0 ± 0.6
Temperature sensitivity of total active season length		3.3	2.9	7.0
Projected active season extension (days)				
RCP 4.5	Extension by 2055	6 ± 2	5 ± 2	13 ± 4
	Extension by 2095	9 ± 2	7 ± 2	18 ± 5
RCP 8.5	Extension by 2055	9 ± 2	8 ± 1	19 ± 3
	Extension by 2095	20 ± 4	17 ± 3	41 ± 8

The model is based on linear extrapolation of experimental results, using CMIP5 climate projections. Temperature sensitivities are derived from Fig. 2; total projected active season extension is the product of the temperature sensitivity of total active season length multiplied by the mean projected temperature increase (decadal means, relative to 2006–2015). Uncertainties in active season extension represent the uncertainty in the climate projections (s.d. across ten models) rather than the uncertainty in the temperature sensitivities.

Extended Data Table 4 | Effect of SPRUCE warming treatments on observed vegetative and reproductive phenological transitions (2016)

			Linear temperature model				Breakpoint temperature model			
Species	Phenophase	Mean DOY	Pearson *r*	RMSE	Slope ± SE	T effect	RMSE	Slope ± SE	*t** ± SE	ΔAICc
Picea mariana	Buds breaking	140 ± 10	0.97	2.8	-2.72 ± 0.23	P < 0.0001	2.9	-2.87 ± 0.31	7.73 ± 0.98	+4.5
(Black spruce, evergreen tree)	Shoots elongating	142 ± 9	0.93	3.6	-2.35 ± 0.29	P < 0.0001	-	-	-	-
Larix laricina	Buds breaking	95 ± 15	0.98	3.6	-4.06 ± 0.29	P < 0.0001	3.3	-4.42 ± 0.35	7.30 ± 0.71	+1.7
(Eastern tamarack, deciduous tree)	Leaves growing	110 ± 10	0.93	3.8	-2.45 ± 0.30	P < 0.0001	3.8	-2.66 ± 0.40	7.31 ± 1.34	+3.8
	Shoots elongating	149 ± 16	0.94	6.0	-4.13 ± 0.49	P < 0.0001	-	-	-	-
C. calyculata	Flowering	110 ± 10	0.97	2.7	-2.63 ± 0.22	P < 0.0001	2.4	-2.93 ± 0.25	6.97 ± 0.75	+0.9
(Leatherleaf, evergreen shrub)	Leaves growing	126 ± 18	0.91	7.6	-4.33 ± 0.62	P < 0.0001	6.1	-6.01 ± 0.90	5.18 ± 0.85	-1.7
	Shoots elongating	128 ± 17	0.93	6.7	-4.37 ± 0.55	P < 0.0001	6.8	-4.78 ± 0.72	7.26 ± 1.32	+3.6
	Flowering (2nd obs.)	108 ± 10	0.83	6.1	-2.00 ± 0.61	P = 0.02	-	-	-	-
Kalmia polifolia	Flowering	129 ± 14	0.75	10.0	-2.83 ± 0.84	P < 0.01	9.4	-5.57 ± 2.18	3.26 ± 1.55	+2.5
(Bog laurel, evergreen shrub)	Flowering (2nd obs.)	125 ± 15	0.95	5.4	-3.18 ± 0.48	P < 0.01	-	-	-	-
R. groenlandicum	Buds breaking	121 ± 10	0.92	4.3	-2.53 ± 0.35	P < 0.0001	-	-	-	-
(Labrador tea, evergreen shrub)	Leaves growing	127 ± 13	0.89	6.2	-3.12 ± 0.51	P < 0.001	-	-	-	-
	Shoots elongating	129 ± 14	0.86	7.7	-3.26 ± 0.62	P < 0.001	6.9	-4.64 ± 1.02	5.01 ± 1.22	+1.0
	Flowering	130 ± 15	0.92	6.2	-3.65 ± 0.50	P < 0.0001	5.9	-5.03 ± 0.86	5.05 ± 0.95	+2.1
	Flowering (2nd obs.)	121 ± 16	1.00	0.7	-3.56 ± 0.06	P < 0.0001	0.6	-3.61 ± 0.06	8.36 ± 0.19	+9.7
V. angustifolium	Buds breaking	117 ± 13	0.98	2.8	-3.34 ± 0.25	P < 0.0001	2.9	-3.61 ± 0.42	7.69 ± 0.98	+5.1
(Lowbush blueberry, deciduous shrub)	Leaves growing	119 ± 13	0.87	6.8	-3.08 ± 0.55	P < 0.001	-	-	-	-
	Flowering	119 ± 11	0.96	3.3	-2.84 ± 0.27	P < 0.0001	3.4	-2.99 ± 0.36	7.78 ± 1.09	+4.1
Eriophorum spp.	Flowering	107 ± 5	0.74	3.6	-1.03 ± 0.29	P < 0.01	-	-	-	-
(Cottongrass, sedge)	Seeds formed	124 ± 10	0.96	2.9	-2.56 ± 0.24	P < 0.0001	-	-	-	-
M.trifolium	Leaves growing	137 ± 13	0.87	6.5	-2.95 ± 0.53	P < 0.001	6.5	-3.41 ± 0.78	6.52 ± 1.65	+3.4
(False Solomon's seal, perennial herb)	Flowering	148 ± 9	0.86	4.8	-2.06 ± 0.39	P < 0.001	5.0	-2.23 ± 0.53	7.37 ± 2.12	+4.4

Data are from 2016 growing season, based on observations across $n = 12$ plots. Species are ordered by functional type, and within each species, phenophases are ordered according to the mean (± 1 s.d.) day of year (DOY) on which the event occurred. Statistics for the linear temperature model are based on regression of transition date (y) on warming treatment (x), and the model slope is the phenological temperature sensitivity in days per 1 °C warming. The '*T* effect' column reports the *P* value for the null hypothesis of no temperature effect. Statistics for the breakpoint temperature model are based on a model in which the response to warming treatment is assumed to be linear up to a temperature threshold t^*, and flat thereafter (see Methods for additional details). No statistics are reported for cases in which a t^* could not be identified, or where the addition of t^* did not improve model fit. ΔAIC_C is the difference in AIC (corrected for small sample sizes) between the linear temperature model and breakpoint temperature model, with a positive value indicating that the linear temperature model is better supported by the data, and a negative value indicating that the breakpoint temperature model is better supported by the data. RMSE, root mean squared error. SE, standard error.

Extended Data Table 5 | Effect of SPRUCE warming treatments on observed vegetative and reproductive phenological transitions (2017)

			Linear Temperature Model				Breakpoint Temperature Model			
Species	Phenophase	Mean DOY	Pearson *r*	RMSE	Slope ± SE	T effect	RMSE	Slope ± SE	*t** ± SE	ΔAICc
C. calyculata	Flowering	107 ± 6	0.91	3.0	-1.46 ± 0.21	P < 0.0001	-	-	-	-
	Leaves growing	134 ± 25	0.90	11.0	-5.75 ± 0.88	P < 0.0001	8.3	-7.41 ± 1.22	6.26 ± 1.06	-3.6
	Shoots elongating	143 ± 20	0.95	7.0	-4.85 ± 0.52	P < 0.0001	7.0	-4.91 ± 0.72	8.76 ± 1.44	+4.7
	Fruiting	147 ± 5	0.71	3.0	-0.86 ± 0.27	P = 0.01	3.3	-1.45 ± 0.78	4.31 ± 2.53	+2.5
	Flowers terminated	159 ± 11	0.78	7.0	-2.17 ± 0.55	P < 0.01	-	-	-	-
	Fall buds	249 ± 0	0.00	0.0	0.00 ± 0.00	-	-	-	-	-
	Leaves colored	310 ± 11	0.88	5.0	2.48 ± 0.42	P < 0.001	3.5	5.79 ± 0.82	2.69 ± 0.49	-6.9
Eriophorum spp.	Leaves greening	105 ± 16	0.81	10.0	-3.38 ± 0.78	P < 0.01	8.4	-5.39 ± 1.23	4.77 ± 1.23	-0.8
	Flowering	106 ± 9	0.66	7.0	-1.50 ± 0.54	P = 0.02	-	-	-	-
	Fruiting	143 ± 24	0.66	19.0	-4.15 ± 1.48	P = 0.02	-	-	-	-
	Flowers terminated	187 ± 29	0.16	30.0	-1.21 ± 2.36	P = 0.62	-	-	-	-
Kalmia polifolia	Leaves greening	113 ± 29	0.82	17.0	-6.22 ± 1.35	P < 0.01	13.8	-12.43 ± 3.23	3.50 ± 1.05	-1.9
	Flowering	120 ± 14	0.95	5.0	-3.38 ± 0.35	P < 0.0001	3.6	-4.52 ± 0.53	5.67 ± 0.70	-2.0
	Leaves growing	135 ± 20	0.57	17.0	-2.96 ± 1.35	P = 0.05	-	-	-	-
	Fruiting	153 ± 11	0.77	7.0	-2.31 ± 0.63	P < 0.01	-	-	-	-
	Flowers terminated	158 ± 9	0.89	4.0	-1.99 ± 0.32	P < 0.0001	-	-	-	-
Larix laricina	Leaves growing	110 ± 11	0.84	6.0	-2.30 ± 0.47	P < 0.001	3.9	-4.93 ± 0.91	3.27 ± 0.71	-7.0
	Shoots elongating	147 ± 11	0.93	4.0	-2.72 ± 0.33	P < 0.0001	4.3	-2.95 ± 0.44	7.76 ± 1.38	+3.9
	Fall buds	260 ± 22	0.31	23.0	-1.78 ± 1.96	P = 0.39	-	-	-	-
	Leaves yellow	300 ± 12	0.94	4.0	2.85 ± 0.33	P < 0.0001	-	-	-	-
	Leaves dropped	318 ± 16	0.93	6.0	3.91 ± 0.49	P < 0.0001	-	-	-	-
M. trifolium	Leaves growing	135 ± 9	0.92	4.0	-2.12 ± 0.28	P < 0.0001	-	-	-	-
	Flowering	140 ± 8	0.90	4.0	-1.94 ± 0.30	P < 0.0001	3.3	-3.99 ± 0.77	3.10 ± 0.72	-0.4
	Fruiting	162 ± 8	0.12	9.0	-0.27 ± 0.74	P = 0.73	-	-	-	-
	Flowers terminated	202 ± 23	0.13	24.0	0.76 ± 1.85	P = 0.69	-	-	-	-
	Leaves senesced	294 ± 17	0.62	14.0	2.84 ± 1.21	P = 0.04	-	-	-	-
Picea mariana	Cones open	134 ± 24	0.82	14.0	-5.01 ± 1.11	P < 0.01	14.8	-5.36 ± 1.53	7.97 ± 2.66	+4.5
	Leaves growing	143 ± 14	0.93	5.0	-3.31 ± 0.41	P < 0.0001	4.9	-4.58 ± 0.72	5.34 ± 0.91	+1.8
	Shoots elongating	155 ± 11	0.91	5.0	-2.64 ± 0.39	P < 0.0001	3.6	-4.13 ± 0.52	4.66 ± 0.67	-4.9
	Fall buds	249 ± 0	0.00	0.0	0.00 ± 0.00	-	-	-	-	-
R. groenlandicum	Flowering	126 ± 15	0.98	3.0	-3.83 ± 0.27	P < 0.0001	3.6	-3.95 ± 0.37	8.47 ± 0.91	+4.3
	Leaves growing	134 ± 11	0.79	7.0	-2.34 ± 0.57	P < 0.01	7.0	-2.83 ± 0.73	6.85 ± 2.23	+2.6
	Shoots elongating	136 ± 14	0.98	3.0	-3.56 ± 0.25	P < 0.0001	2.6	-4.00 ± 0.27	7.30 ± 0.60	-1.7
	Fruiting	154 ± 9	0.96	3.0	-2.28 ± 0.21	P < 0.0001	2.4	-2.62 ± 0.24	7.02 ± 0.82	-0.1
	Flowers terminated	167 ± 7	0.87	4.0	-1.59 ± 0.28	P < 0.001	-	-	-	-
	Last flowers (2nd flush)	277 ± 44	0.74	32.0	9.33 ± 3.22	P = 0.02	-	-	-	-
	Leaves folding	307 ± 19	0.84	11.0	4.06 ± 0.84	P < 0.001	9.8	4.93 ± 1.44	6.77 ± 1.99	+1.2
V. angustifolium	Leaves growing	118 ± 15	0.90	7.0	-3.54 ± 0.55	P < 0.0001	5.7	-4.90 ± 0.83	5.60 ± 1.01	-1.7
	Flowering	120 ± 15	0.85	8.0	-3.23 ± 0.62	P < 0.001	8.4	-3.33 ± 0.86	8.47 ± 2.49	+4.7
	Shoots elongating	140 ± 25	0.75	17.0	-4.66 ± 1.36	P < 0.01	-	-	-	-
	Fruiting	145 ± 15	0.69	11.0	-2.65 ± 0.88	P = 0.01	11.6	-3.07 ± 1.20	6.86 ± 3.39	+4.3
	Flowers terminated	161 ± 15	0.67	11.0	-2.51 ± 0.89	P = 0.02	11.3	-3.94 ± 1.93	4.65 ± 2.49	+3.4
	Fruits ripened	181 ± 15	0.90	7.0	-3.57 ± 0.59	P < 0.001	4.6	-5.84 ± 1.08	4.18 ± 0.88	-2.9
	Leaves colored	303 ± 19	0.01	20.0	0.04 ± 1.54	P = 0.98	-	-	-	-

Data are from the 2017 growing season, based on observations across $n = 12$ plots. Species are ordered alphabetically, and within each species, phenophases are ordered according to the mean (± 1 s.d.) day of year (DOY) on which the event occurred. Statistics for the linear temperature model are based on regression of transition date (y) on warming treatment (x), and the model slope is the phenological temperature sensitivity in days per 1 °C warming. The '*T* effect' column reports the *P* value for the null hypothesis of no temperature effect. Statistics for the breakpoint temperature model are based on a model in which the response to warming treatment is assumed to be linear up to a temperature threshold t^*, and flat thereafter (see Methods for additional details). No statistics are reported for cases in which a t^* could not be identified, or where the addition of t^* did not improve model fit. ΔAIC_C is the difference in AIC (corrected for small sample sizes) between the linear temperature model and breakpoint temperature model, with a positive value indicating that the linear temperature model is better supported by the data, and a negative value indicating that the breakpoint temperature model is better supported by the data. RMSE, root mean squared error. SE, standard error. Results not shown for the linear temperature and CO_2 model as the CO_2 effect and $CO_2 \times T$ interaction effect were generally not significant (see Supplementary Note 5 for additional information).

Extended Data Table 6 | Impact of premature foliar senescence on nutrient content of *L. laricina* and *P. mariana* litter

		Larix laricina		*Picea mariana*	
		mean	range	mean	range
Spring, post-frost	N (%)	1.79	(0.71-2.85)	0.71	(0.43-0.83)
Premature senescent litter	C (%)	46.2	(46.1-46.3)	46.3	(44.7-50.0)
Fall	N (%)	0.35	(0.30-0.40)	0.42	(0.34-0.50)
Normal senescent litter	C (%)	51.1	(50.9-51.4)	51.8	(51.1-52.5)
Senescent litter ratio	N_{pre}:N_{norm}	5.11		1.69	
Premature:Normal	C_{pre}:C_{norm}	0.90		0.89	

Following the 9 April 2016 spring frost event, damaged foliage from trees that had lost frost hardiness began a period of senescence, culminating in heavy leaf fall during early May as air temperatures frequently exceeded 30 °C in the +9.0 °C plots (temperatures over 40 °C were observed in plot 10 and plot 17 on 5 and 6 May). Prematurely senescent litter was collected on 6 May from the ground underneath damaged trees in the two warmest treatments (+6.75 and +9.0 °C) (n = 3–7 trees). Normally senescent litter was collected on 4 November from ambient environment plots outside of the experimental treatments using litter baskets (n = 8 trees). Litter was analysed for carbon and nitrogen by combustion using 0.1-g samples of oven-dried and finely ground tissue on a TruSpec elemental analyser (LECO). Data are presented on a per cent dry matter basis.

nature research

Corresponding author(s): Andrew D. Richardson

Reporting Summary

Nature Research wishes to improve the reproducibility of the work that we publish. This form provides structure for consistency and transparency in reporting. For further information on Nature Research policies, see Authors & Referees and the Editorial Policy Checklist.

Statistical parameters

When statistical analyses are reported, confirm that the following items are present in the relevant location (e.g. figure legend, table legend, main text, or Methods section).

n/a	Confirmed	
☐	☒	The exact sample size (*n*) for each experimental group/condition, given as a discrete number and unit of measurement
☐	☒	An indication of whether measurements were taken from distinct samples or whether the same sample was measured repeatedly
☐	☒	The statistical test(s) used AND whether they are one- or two-sided *Only common tests should be described solely by name; describe more complex techniques in the Methods section.*
☐	☒	A description of all covariates tested
☒	☐	A description of any assumptions or corrections, such as tests of normality and adjustment for multiple comparisons
☐	☒	A full description of the statistics including central tendency (e.g. means) or other basic estimates (e.g. regression coefficient) AND variation (e.g. standard deviation) or associated estimates of uncertainty (e.g. confidence intervals)
☐	☒	For null hypothesis testing, the test statistic (e.g. *F*, *t*, *r*) with confidence intervals, effect sizes, degrees of freedom and *P* value noted *Give P values as exact values whenever suitable.*
☒	☐	For Bayesian analysis, information on the choice of priors and Markov chain Monte Carlo settings
☒	☐	For hierarchical and complex designs, identification of the appropriate level for tests and full reporting of outcomes
☐	☒	Estimates of effect sizes (e.g. Cohen's *d*, Pearson's *r*), indicating how they were calculated
☐	☒	Clearly defined error bars *State explicitly what error bars represent (e.g. SD, SE, CI)*

Our web collection on statistics for biologists may be useful.

Software and code

Policy information about availability of computer code

Data collection	PhenoCam imagery and data processed as described in Richardson et al. (2018) Scientific Data 5: 180028. Links to processing code on GitHub are contained in this paper.
Data analysis	Data analysis conducted in SAS v9

For manuscripts utilizing custom algorithms or software that are central to the research but not yet described in published literature, software must be made available to editors/reviewers upon request. We strongly encourage code deposition in a community repository (e.g. GitHub). See the Nature Research guidelines for submitting code & software for further information.

Data

Policy information about availability of data

All manuscripts must include a data availability statement. This statement should provide the following information, where applicable:

- Accession codes, unique identifiers, or web links for publicly available datasets
- A list of figures that have associated raw data
- A description of any restrictions on data availability

All data are publicly available. PhenoCam imagery is publicly available through the project web page (http://phenocam.sr.unh.edu), and the phenological data sets used in this study are available through the SPRUCE data portal, https://doi.org/10.3334/CDIAC/spruce.045 and https://doi.org/10.3334/CDIAC/spruce.044.

Field-specific reporting

Please select the best fit for your research. If you are not sure, read the appropriate sections before making your selection.

☐ Life sciences ☐ Behavioural & social sciences ☒ Ecological, evolutionary & environmental sciences

For a reference copy of the document with all sections, see nature.com/authors/policies/ReportingSummary-flat.pdf

Ecological, evolutionary & environmental sciences study design

All studies must disclose on these points even when the disclosure is negative.

Study description	There are 10 experimental enclosures. The experiment uses a regression-based design, with 5 levels of warming from +0 (control) to +9 °C, in 2.25 °C increments. Thus each level of warming is replicated twice. The temperature treatments are crossed with a CO2 treatment, so that at each level of warming, one replicate receives ambient CO2 and the other replicate receives elevated CO2. Thus 5 of the 10 enclosures receive elevated CO2. Treatments were randomly assigned, and treatments were independently applied to each enclosure. Thus an enclosure is an experimental unit. For further details, see Hanson et al (2017) Biogeosciences 14: 861-883. Our analysis treats temperature as a continuous variable and CO2 as a class variable with two levels (elevated and ambient). In testing for temperature effects, we evaluate both linear and breakpoint models, as described in Methods. In testing CO2 effects, we include both CO2 and a CO2 x temperature interaction effect.
Research sample	Observations were conducted at the species level within each enclosure. Because most species were found in each of the 10 enclosures, we consider the sample size to be n = 10. An exception is Larix, which was not visible in the camera imagery for one enclosure. Hence for this species, n = 9 for the camera data.
Sampling strategy	Statistical methods were not used to predetermine sample size. The range of temperatures applied was selected to ensure that at least the warmest enclosures exceed model-based projections of future temperature increase expected by 2100. Financial considerations precluded additional replication at each level of warming.
Data collection	Phenological ground observations were conducted by WRN and RRH, with data recorded (was a particular phenophase observed, yes or no?) on a pre-printed form for each enclosure ADR transcribed the data and determined phenological transition dates, based on the first "yes" observation following a series of "no" observations. PhenoCam imagery was recorded automatically every 30 minutes from 4 am to 10 pm, following standard PhenoCam procedures (as described in Richardson et al. (2018) Scientific Data). ADR drew the masks used to define the three vegetation types for which data was extracted. Automated image processing and extraction of phenological transition dates follows Richardson et al (2018) Scientific Data.
Timing and spatial scale	Phenological ground observations were conducted in Spring 2016 (April to July) and Spring and Autumn 2017 (April to December), at approximately weekly intervals. While twice-weekly surveys would have been ideal, and would have enabled more precise identification of transition dates, the observers had other duties at the site which made more frequent observations impossible. Ground observations represent the consensus across multiple individuals of a species within each enclosure. PhenoCam imagery was recorded automatically every 30 minutes from 4 am to 10 pm, beginning August 2015. Here we use data through December 2017 but note that image acquisition is ongoing.
Data exclusions	For the ground observations of phenology, the rationale for excluding some phenophases from the analysis is described in Methods. Briefly, for certain phenophases for certain species, the observers felt either that (1) the phenophase was difficult to observe reliably or (2) the species was not sufficiently well distributed for the observations to be robust. No individual data points were excluded. No data were excluded from PhenoCam observations.
Reproducibility	Due to costs, full replication of the experiment was not feasible. Instead, we show that the observed patterns are consistent from year-to-year over the 2.5 y (to date) of the experiment, and consistent between ground observations and PhenoCam data. The experiment is scheduled to run for 10 y.
Randomization	17 permanent plots were established within the SPRUCE S1 bog in 2012. Assignment of the experimental treatments to 10 of these permanent plots was random. See Hanson et al. (2017) Biogeosciences for additional details.
Blinding	Blinding is not feasible. It is impossible for observers not to be aware of the temperature treatments in each enclosure.

Did the study involve field work? ☒ Yes ☐ No

Field work, collection and transport

Field conditions	The historic climate at the site is subhumid continental: mean annual temperature is 4°C, mean annual precipitation is 750 mm, and extreme temperatures range from –38 °C to +30 °C. Temperatures in the warmest (+9 °C) enclosures exceed those in the

	control (+0 °C) enclosures by the target amount. Temperatures in the control enclosures exceed ambient temperatures by 1-2 ° C.
Location	The SPRUCE experiment is conducted at the Marcell Experimental Forest, near Grand Rapids, Minnesota, USA ((47° 30.171' N, 93° 28.970' W), on land owned by the US Forest Service.
Access and import/export	The SPRUCE experiment is a collaborative effort between DOE's Oak Ridge National Laboratory (operated by UT-Battelle) and the US Forest Service's (USFS) Northern Research Station, conducted under a memorandum of understanding between UT-Battelle and the Forest Service dated 11/03/2009. DOE completed an Environmental Assessment (DOE/EA-1764) and DOE and USFS determined that the "proposed action is not a major federal action that would significantly affect the quality of the human environment within the meaning of the National Environmental Protection Act (NEPA) of 1969". Therefore, based on the "finding of no significant impact", the preparation of an Environmental Impact Statement was not necessary.
Disturbance	A geotechnical site survey was completed in 2011 by American Engineering Testing, Inc. (report 07-05001). Prior to the installation of the experimental enclosures, a network of raised boardwalks was constructed to minimize disturbance and damage to the site. Within each enclosure a circular boardwalk permits access to vegetation without trampling or further disturbance. Potential artifacts associated with the construction of the enclosures are discussed by Hanson et al. (2017) Biogeosciences.

Reporting for specific materials, systems and methods

Materials & experimental systems

n/a	Involved in the study
☒	☐ Unique biological materials
☒	☐ Antibodies
☒	☐ Eukaryotic cell lines
☒	☐ Palaeontology
☒	☐ Animals and other organisms
☒	☐ Human research participants

Methods

n/a	Involved in the study
☒	☐ ChIP-seq
☒	☐ Flow cytometry
☒	☐ MRI-based neuroimaging